Molecular excited states from the SCAN functional

David J. Tozer[1] and Michael J. G. Peach[2]

1. Department of Chemistry, Durham University, South Road, Durham, DH1 3LE, UK

2. Department of Chemistry, Lancaster University, Lancaster, LA1 4YB, UK

March 1, 2018

The performance of the strongly constrained and appropriately normed (SCAN) [Phys. Rev. Lett. **115**, 036402 (2015)] meta-generalised gradient approximation exchange–correlation functional is investigated for the calculation of time-dependent density-functional theory (TDDFT) molecular excitation energies of local, charge-transfer, and Rydberg character, together with the excited $^3\Sigma_u^+$ potential energy curve in H_2. The SCAN results frequently resemble those obtained using a global hybrid functional, with either a standard or increased fraction of exact orbital exchange. For local excitations, SCAN can exhibit significant triplet instability problems, resulting in imaginary triplet excitation energies for a number of cases. The Tamm–Dancoff approximation offers a simple approach to improve the situation, but the excitation energies are still significantly underestimated. Understanding the origin of these (near)-triplet instabilities may provide useful insight into future functional development.

1 Introduction

The strongly constrained and appropriately normed (SCAN) functional of Sun *et al.* [1] is the state-of-the-art, non-empirical, semi-local exchange–correlation functional in density-functional theory [2, 3] (DFT). As a meta-GGA (meta-generalised gradient approximation), it depends not only on the density and the reduced density gradient as conventional GGA functionals, but also on the kinetic energy density. This dependence provides additional flexibility that allows the functional form to satisfy additional constraints.

Developed from first principles, SCAN satisfies all of the exact constraints that it is possible for a meta-GGA to satisfy [1]. When applied to an extensive variety of problems in solid state physics (see e.g., Refs. [4–8] for some recent examples), this functional has demonstrated improved performance over previous semi-local functionals (either at the GGA or meta-GGA level), perhaps suggesting that it has introduced additional 'physics' through its more constrained form.

There have also been a limited number of assessments of the functional applied to molecular systems [9–12], focusing on ground state properties, where there are again indications that it does not behave as a prototypical semi-local functional. In particular, observations around its hybrid-like performance for an extensive set of atomisation energies and related ground state properties [13], are indicative of the SCAN functional reproducing aspects of the underlying behaviour attributed to global hybrid functionals.

Our interest here lies in the properties of excited states of singlet ground-state molecules from time-dependent DFT [14, 15] (TDDFT) within the adiabatic approximation. For local excitations, special attention must be paid to the possible effect of triplet (near)-instabilities [16–23], which can be identified by calculating the triplet stability, $\omega_{\rm stab}$. This quantifies the stability of the Kohn–Sham determinant with respect to spin-symmetry breaking orbital rotations [24–26]. Small positive values of $\omega_{\rm stab}$ indicate near-instabilities and correlate with underestimated triplet TDDFT excitation energies; negative values indicate actual instabilities and lead to imaginary triplet TDDFT excitation energies [21]. It is well established [17, 19, 21–23, 27–32] that application of the Tamm–Dancoff approximation [33, 34] (TDA) largely repairs the problem with conventional functionals, and so the magnitude of the difference between TDA and TDDFT excitation energies provides an alternative measure of the effect of triplet (near)-instabilities [21, 22].

In Ref. [21], we demonstrated that for TDDFT excitations from singlet ground state to triplet local excited states, the effect of triplet (near)-instabilities

became increasingly pronounced as the fraction of exact orbital exchange in the functional increases. Interestingly, TDDFT excitations to the spatially equivalent *singlet* states (i.e., those states involving the same dominant orbital rotations) could also be affected, although the effect became *less* pronounced as the fraction of exact orbital exchange increases. It is therefore of interest to establish whether the hybrid-like behaviour of SCAN noted in Ref. [13] is evident in the context of the triplet instability.

We also consider excited states of charge-transfer and Rydberg character. For both categories, it is well-established that increasing the fraction of exact orbital exchange reduces the errors and so it is again informative to investigate the performance of SCAN.

We consider a series of representative local, charge-transfer and Rydberg excitation energies, of both singlet and triplet spin (from singlet ground state molecules), together with the $^3\Sigma_u^+$ excited state surface in H_2. We compare the results from SCAN with those from the Perdew–Burke–Ernzerhof [35] (PBE) GGA and the Becke-3 parameter hybrid functional with Lee–Yang–Parr correlation [36–40] (B3LYP) containing a fixed 20% exact orbital exchange, and discuss the results in the context of triplet stability, ω_{stab}. Computational Details are discussed in Section 2 and Results and Discussion are presented in Section 3. Conclusions are presented in Section 4.

2 Computational Details

All SCAN calculations were undertaken with the Q-Chem 5.0 program [41]. For the other functionals, calculations were undertaken with a combination of Q-Chem 5.0, Dalton 15 [42, 43], and Gaussian 09 [44]. Throughout, we use the standard generalised Kohn–Sham formalism. Here, the exchange–correlation (XC) potential and kernel contributions corresponding to any orbital-dependent components (i.e., the exact orbital exchange contributions in hybrid functionals, and the kinetic energy density contributions in meta-GGAs) are evaluated as derivatives with respect to the Kohn–Sham orbitals, rather than the density. This is the conventional approach for ground and excited state calculations within DFT, (for a discussion of this approach in the context of meta-GGA functionals and excited states, see ref [45]).

We use a large numerical integration quadrature grid for evaluating the exchange–correlation energy contributions (as necessitated by the kinetic energy density component of the SCAN functional), and have confirmed that our observations are independent of making the quadrature even more extensive. With the exception of the diatomic molecules, the aug-cc-pVTZ basis set [46, 47] is used for all DFT calculations. For CO and N_2, we use the d-aug-cc-pVTZ basis set [46, 47], due to the consideration of high-lying Rydberg excited states therein. For H_2, we use the cc-pVTZ basis set [46] to minimise convergence issues at small interatomic distances.

For CO and N_2, we use experimental geometries and compare with reference results [22] from d-aug-cc-pVTZ approximate third order coupled cluster theory, CC3 [48, 49]. For the other molecules, we use the geometries as defined in the original studies from which we have taken the molecules; we also use the same reference data. Specifically, for acetamide and propanamide, MP2/6-31G* geometries are used following Ref. [50], and we compare our DFT excitation energies with the theoretical best estimates (complete active space self-consistent field with second order perturbation theory correction, CASPT2 [51, 52], and CC3) taken from the work of Thiel and co-workers in Refs. [50, 53–55]. Following Ref. [56], we use CAM-B3LYP [57]/6-31G* geometries for the polyacetylene oligomer (PAO) series, the B3LYP/TZVP geometry for naphthalene, and the MP2/6-31G* geometry for the model dipeptide. In each of these cases, we compare our DFT excitation energies with equations of motion coupled cluster with single and double excitations [58, 59] (EOM-CCSD) excitation energies evaluated in the cc-pVTZ basis set, with a correction to account for the influence of diffuse functions [22]. The H_2 results are compared with CCSD (full configuration-interaction) results.

For all the molecules that we consider, the triplet states we investigate are of equivalent character to the singlet states (i.e., the character/dominant orbital rotations are the same, irrespective of spin).

3 Results and Discussion

We begin by examining a selection of excitation energies in small molecules. The molecules have been selected on the basis of being representative of that class of excitations within the larger benchmark sets

from which they have been taken. All excitation energies discussed are presented in table 1.

3.1 Local excitations

First, we consider two low-lying excitations in acetamide and propanamide, paying attention to whether the system-dependence of the reference excitation energies can be reproduced. For the singlets, the $^1A''$ excitation energy increases slightly between acetamide and propanamide, whereas the $^1A'$ state excitation energy drops slightly. For the triplets, both excitation energies increase between acetamide and propanamide, with the change being particularly pronounced for the $^3A'$ state.

First consider the singlet excitations determined using TDDFT. All three functionals correctly reproduce the trend between the two molecules for both states. For PBE, the excitation energies underestimate the reference values by at least 0.4 eV, which is typical behaviour for local excitations. With B3LYP, each of the excitation energies increases, reducing the error relative to reference values. However, all of the excitations remain underestimated. With SCAN, there is a further increase in excitation energies, and the values are now overestimated, by between 0.1 – 0.2 eV. This is comparable to the behaviour of a hybrid functional with a significant amount of exact orbital exchange. The influence of the TDA is very small for all three functionals (< 0.1 eV).

Next consider the triplet excitations determined using TDDFT. The increase in the reference $^3A''$ excitation energy is correctly reproduced by all three functionals, whereas the notable increase in the $^3A'$ energy is not reproduced by any of them. The excitation energies again increase from PBE to B3LYP to SCAN, but this time SCAN does not overestimate the reference values. The influence of the TDA is still relatively small, but it is more pronounced than it was for the singlets. Its influence increases from PBE to B3LYP to SCAN, meaning the behaviour of SCAN is again comparable to that of a hybrid functional with a significant amount of exact orbital exchange (in the context of Ref. [22]).

Next, we consider a series of polyacetylene oligomers, with between 2 and 5 repeat units (PAO-2 to PAO-5), focussing on the lowest state of B_u symmetry. For both singlets and triplets, the reference excitation energy decreases notably as the number of repeat units increases across the series.

For the TDDFT singlet excitations, all three functionals reproduce the basic trend of decreasing excitation energy with increasing chain length across the series. With PBE, the excitation energies are all underestimated, quite significantly (and increasingly so across the series). Similar results are observed with B3LYP, although in each case the excitations are closer to the reference values. The SCAN results are very close to those obtained using B3LYP.

The effect of the TDA is now significant, improving the accuracy in all cases. Its effect is less pronounced for B3LYP and SCAN than it is for PBE, meaning the behaviour of SCAN is again comparable to that of a hybrid functional, in the context of Ref. [22].

For the TDDFT triplet excitations, the trend across the series is reproduced with PBE and B3LYP. The PBE values are again too low. In moving to B3LYP, however, the underestimation *increases*, which contrasts the behaviour for the singlet states. In moving to SCAN, the excitation energies become imaginary! (Imaginary excitations are indicated with a dash in the table). These observations (and those for the singlet states, above) are easily understood from the ω_{stab} values, which have average values (over the series) of $+1.7$ eV, $+1.3$ eV, and -0.7 eV for PBE, B3LYP, and SCAN, respectively. Once again, SCAN is exhibiting hybrid-like behaviour with a large fraction of exchange. The effect of the TDA is therefore again increasingly pronounced from PBE to B3LYP to SCAN, improving accuracy for all three functionals and leading to real (and thus physically meaningful, albeit relatively inaccurate) excitation energies with SCAN.

The final set of local excitations we consider are the B_{2u} and B_{3u} excitations in naphthalene and the results are fully consistent with those discussed above. It has been widely observed that many DFT functionals incorrectly predict the state ordering of the two singlet states; the $^1B_{3u}$ state should be lower in energy than the $^1B_{2u}$ state [56, 60].

For the TDDFT singlet excitations, all three functionals yield the incorrect state ordering, due to a notable underestimation of the $^1B_{2u}$ state energy. The SCAN results are again similar to B3LYP and are an improvement over PBE. The effect of the TDA is more pronounced for the $^1B_{2u}$ state than the $^1B_{3u}$ state meaning the state ordering is corrected by TDA

for PBE and B3LYP. However, the influence is insufficient to correct the SCAN state ordering. In moving from PBE to B3LYP, the TDDFT $^3B_{3u}$ excitation energy increases, whereas for the $^3B_{2u}$ state, it reduces. For SCAN, the $^3B_{2u}$ state excitation energy is imaginary. Note that, due to this imaginary value, it was not possible to calculate the SCAN $^3B_{3u}$ value and so it is omitted from the table. Again, the observations are easily understood in terms of ω_{stab}, which is notably lower for the $^3B_{2u}$ state, reducing from +2.2 eV to +1.8 eV to −0.4 eV for PBE, B3LYP, and SCAN, respectively. Application of the TDA improves matters significantly, (necessarily) yielding a real SCAN excitation energy, although the accuracy remains poor.

We find that for naphthalene and the PAO oligomers, the smallest singlet–triplet energy difference computed using SCF energies is significantly lower when computed with SCAN as compared to both PBE and B3LYP, consistent with the observed behaviour with the TDA excitation energies.

As highlighted in section 2, our calculations employ the conventional GKS formalism. The alternative is to use the optimised effective potential (OEP) approach, where *all* XC potential and kernel contributions are evaluated via derivatives with respect to the density. We note that in the context of exact-exchange only OEP, Hirata et al.[61] found that excitation energies in the presence of triplet instabilities are barely affected by the switch to an OEP formalism. Importantly, they showed that the use of the TDA is still required to obtain physically meaningful excitations in situations strongly affected by triplet instability problems. This is consistent with the view that whilst the triplet instability problem manifests in excitation energies, it is fundamentally a failure of the ground state.

3.2 Charge-Transfer Excitations

When considering charge-transfer excitations, although hybrid functionals offer an improvement over conventional semi-local functionals, in these cases standard hybrid functionals are still poor relative to reference values or the results achievable by range-separated hybrid/Coulomb-attenuated functionals [56]. This relates to the need to describe 'separated charge' interactions, that are formally only correctly captured by 100% exact orbital exchange [62].

To probe the performance of SCAN for CT states, we consider a model dipeptide system [22, 56, 63], which exhibits two low-overlap CT excitations of interest. The TDDFT singlet excitations are underestimated with PBE by in excess of 2 eV (with the lower overlap state underestimated by 3.3 eV). The excitations improve with B3LYP, but the maximum underestimation is still 1.7 eV. The SCAN results are intermediate between PBE and B3LYP. The effect of the TDA is small in all cases. Analogous observations are made for the triplet states. From this, it is clear that SCAN is able to reproduce some long-range effects, but still suffers from the standard problems of low-overlap CT, albeit to a lesser extent than with conventional semi-local functionals.

3.3 Rydberg Excitations

The underestimation of Rydberg excitations by conventional semi-local functionals is well-known, due to the incorrect behaviour of the exchange–correlation potential at long-range (which is critical for the highly diffuse orbitals involved in Rydberg excitations) [64, 65]. To probe the behaviour of SCAN for Rydberg excitations, we consider CO and N_2 as prototypical examples, noting that the effect of the TDA is small throughout and that analogous observations are made for the singlet and triplet states.

For both CO and N_2, TDDFT excitation energies from PBE are significantly underestimated, by up to 2 eV. Excitations with B3LYP are improved, but are still significantly underestimated. To correctly describe these states with a conventional hybrid functional, a significant exact orbital exchange contribution (approaching 100%) is required. With the SCAN functional, we find a much larger increase in excitation energy than we have observed with the other molecules examined so far; the average change is to increase over the PBE excitations by 0.7 eV. For CO, this results in a significant improvement and B3LYP-like excitation energies. For N_2, the improvement is less pronounced, however the original underestimation of PBE is more significant.

3.4 The H_2 $^3\Sigma_u^+$ potential energy curve

A key observation in Section 3.1 is that the SCAN functional can be susceptible to triplet instability problems (i.e., as characterised by low or negative

ω_{stab} values), as strikingly illustrated in the polyacetylene oligomers and naphthalene. It is therefore pertinent to end the study with a consideration of the $^3\Sigma_u^+$ potential energy curve in the H_2 molecule, since this is the prototypical example of the triplet instability problem in the context of excited state potential energy surfaces.

The results are as anticipated. Figure 1(a) plots ω_{stab} corresponding to the $^1\Sigma_g^+ \rightarrow {}^3\Sigma_u^+$ excitation for PBE, B3LYP, and SCAN, as a function of bond length, R. (The experimental equilibrium bond length is $R_e = 0.741$ Å). For all but the largest R values, SCAN exhibits the lowest stability. All three stabilities drop with increasing R and the Coulson–Fischer [66] (CF) point (where $\omega_{\text{stab}} = 0$) is shortest with SCAN. The CF points are at 1.451 Å for SCAN, compared to 1.619 and 1.488 Å for PBE and B3LYP, respectively. Figure 1(b) presents the $^3\Sigma_u^+$ TDDFT potential energy curves over the same range of R values, obtained by adding the TDDFT excitation energy to the $^1\Sigma_g^+$ ground state energy. Also shown is the CCSD curve, which is exact within the basis set. As R increases and ω_{stab} decreases towards zero, the excitation energy approaches zero from above and the excited state curve collapses to the ground state at the CF point. At distances beyond the Coulson–Fischer point, the excitation energy is imaginary and so the curve is not plotted. Figure 1(c) presents the TDA potential energy curves, which are real-valued for all R and a significant improvement for all three functionals.

4 Conclusions

We have investigated the performance of the SCAN meta-GGA functional for the calculation of TDDFT molecular excitation energies of local, charge-transfer and Rydberg character, together with the excited $^3\Sigma_u^+$ potential energy curve in H_2. Consistent with the ground state findings of Ref. [13], the SCAN results frequently resemble those obtained using a hybrid functional, with either a standard or increased fraction of exact orbital exchange. For local excitations, SCAN can exhibit significant triplet instability problems, resulting in imaginary triplet excitation energies for a number of cases. The Tamm–Dancoff approximation offers a simple approach to improve matters, but significant underestimation remains. Understanding the origin of these (near)-triplet instabilities may provide useful insight into future functional development. We are presently investigating the performance of a range of meta-GGA functionals in the context of triplet instabilities.

Acknowledgements

MJGP thanks Lancaster University, and the Joy Welch Foundation for financial support. DJT thanks Durham University for financial support.

5 References

References

[1] J. Sun, A. Ruzsinszky and J.P. Perdew, Phys. Rev. Lett. **115**, 036402 (2015).

[2] P. Hohenberg and W. Kohn, Phys. Rev. **136** (3B), B864 (1964).

[3] W. Kohn and L.J. Sham, Phys. Rev. **140** (4A), A1133 (1965).

[4] M. Bokdam, J. Lahnsteiner, B. Ramberger, T. Schäfer and G. Kresse, Phys. Rev. Lett. **119**, 145501 (2017).

[5] B.J. Kennedy, Q. Zhou, S. Zhao, F. Jia, W. Ren and K.S. Knight, Phys. Rev. B **96**, 214105 (2017).

[6] I. Kylänpää, J. Balachandran, P. Ganesh, O. Heinonen, P.R.C. Kent and J.T. Krogel, Phys. Rev. Materials **1**, 065408 (2017).

[7] Y. Yao and Y. Kanai, J. Chem. Phys. **146** (22), 224105 (2017).

[8] Y. Zhang, J. Sun, J.P. Perdew and X. Wu, Phys. Rev. B **96**, 035143 (2017).

[9] J.G. Brandenburg, J.E. Bates, J. Sun and J.P. Perdew, Phys. Rev. B **94**, 115144 (2016).

[10] J. Sun, R.C. Remsing, Y. Zhang, Z. Sun, A. Ruzsinszky, H. Peng, Z. Yang, A. Paul, U. Waghmare, X. Wu, M.L. Klein and J.P. Perdew, Nat. Chem. **8**, 831 (2016).

[11] L. Goerigk, A. Hansen, C. Bauer, S. Ehrlich, A. Najibi and S. Grimme, Phys. Chem. Chem. Phys. **19**, 32184 (2017).

[12] N. Mardirossian and M. Head-Gordon, Mol. Phys. **115** (19), 2315 (2017).

[13] K. Hui and J.D. Chai, J. Chem. Phys. **144** (4), 044114 (2016).

[14] E. Runge and E.K.U. Gross, Phys. Rev. Lett. **52** (12), 997 (1984).

[15] M.E. Casida, in *Recent Advances in Density Functional Methods, Part I*, edited by D. P. Chong (World Scientific, Singapore, 1995), pp. 155–192.

[16] R. Bauernschmitt and R. Ahlrichs, Chem. Phys. Lett. **256** (4–5), 454 (1996).

[17] S. Hirata and M. Head-Gordon, Chem. Phys. Lett. **314** (3–4), 291 (1999).

[18] M.E. Casida, F. Gutierrez, J. Guan, F.X. Gadea, D. Salahub and J.P. Daudey, J. Chem. Phys. **113** (17), 7062 (2000).

[19] F. Cordova, L.J. Doriol, A. Ipatov, M.E. Casida, C. Filippi and A. Vela, J. Chem. Phys. **127** (16), 164111 (2007).

[20] O.B. Lutnæs, T. Helgaker and M. Jaszuński, Mol. Phys. **108** (19), 2579 (2010).

[21] M.J.G. Peach, M.J. Williamson and D.J. Tozer, J. Chem. Theory Comput. **7** (11), 3578 (2011).

[22] M.J.G. Peach and D.J. Tozer, J. Phys. Chem. A **116** (39), 9783 (2012).

[23] M.J.G. Peach, N. Warner and D.J. Tozer, Mol. Phys. **111** (9-11), 1271 (2013).

[24] J. Čížek and J. Paldus, J. Chem. Phys. **47** (10), 3976 (1967).

[25] R. Seeger and J.A. Pople, J. Chem. Phys. **66** (7), 3045 (1977).

[26] R. Bauernschmitt and R. Ahlrichs, J. Chem. Phys. **104** (22), 9047 (1996).

[27] C.P. Hsu, S. Hirata and M. Head-Gordon, J. Phys. Chem. A **105** (2), 451 (2001).

[28] S. Grimme and F. Neese, J. Chem. Phys. **127** (15), 154116 (2007).

[29] Y.L. Wang and G.S. Wu, Int. J. Quantum Chem. **108** (3), 430 (2008).

[30] C. Adamo and D. Jacquemin, Chem. Soc. Rev. **42**, 845 (2013).

[31] A.D. Laurent and D. Jacquemin, Int. J. Quantum Chem. **113** (17), 2019 (2013).

[32] D. Jacquemin, I. Duchemin, A. Blondel and X. Blase, J. Chem. Theory Comput. **13** (2), 767 (2017).

[33] I. Tamm, J. Phys. (USSR) **9**, 449 (1945).

[34] S.M. Dancoff, Phys. Rev. **78** (4), 382 (1950).

[35] J.P. Perdew, K. Burke and M. Ernzerhof, Phys. Rev. Lett. **77** (18), 3865 (1996).

[36] A.D. Becke, Phys. Rev. A **38** (6), 3098 (1988).

[37] A.D. Becke, J. Chem. Phys. **98** (7), 5648 (1993).

[38] S.H. Vosko, L. Wilk and M. Nusair, Can. J. Phys. **58** (8), 1200 (1980).

[39] C. Lee, W. Yang and R.G. Parr, Phys. Rev. B **37** (2), 785 (1988).

[40] P.J. Stephens, F.J. Devlin, C.F. Chabalowski and M.J. Frisch, J. Phys. Chem. **98** (45), 11623 (1994).

[41] Y. Shao, Z. Gan, E. Epifanovsky *et al.*, Mol. Phys. **113** (2), 184 (2015).

[42] K. Aidas, C. Angeli, K.L. Bak, V. Bakken, R. Bast, L. Boman, O. Christiansen, R. Cimiraglia, S. Coriani, P. Dahle, E.K. Dalskov, U. Ekström, T. Enevoldsen, J.J. Eriksen, P. Ettenhuber, B. Fernández, L. Ferrighi, H. Fliegl, L. Frediani, K. Hald, A. Halkier, C. Hättig, H. Heiberg, T. Helgaker, A.C. Hennum, H. Hettema, E. Hjertenæs, S. Høst, I.M. Høyvik, M.F. Iozzi, B. Jansík, H.J.A. Jensen, D. Jonsson, P. Jørgensen, J. Kauczor, S. Kirpekar, T. Kjærgaard, W. Klopper, S. Knecht, R. Kobayashi, H. Koch, J. Kongsted, A. Krapp, K. Kristensen, A. Ligabue, O.B. Lutnæs, J.I. Melo, K.V. Mikkelsen, R.H. Myhre, C. Neiss, C.B. Nielsen, P. Norman, J. Olsen, J.M.H. Olsen, A. Osted, M.J. Packer, F. Pawlowski, T.B. Pedersen, P.F. Provasi, S. Reine, Z. Rinkevicius, T.A. Ruden, K. Ruud, V.V. Rybkin, P. Sałek, C.C.M. Samson, A.S. de Merás, T. Saue, S.P.A. Sauer, B. Schimmelpfennig, K. Sneskov, A.H. Steindal, K.O. Sylvester-Hvid, P.R. Taylor, A.M. Teale, E.I. Tellgren, D.P. Tew, A.J. Thorvaldsen, L.

Thøgersen, O. Vahtras, M.A. Watson, D.J.D. Wilson, M. Ziolkowski and H. Ågren, Wiley Interdiscip. Rev.: Comput. Mol. Sci. **4** (3), 269 (2014).

[43] Dalton, a molecular electronic structure program, Release Dalton2015 2015, Retrieved from <http://daltonprogram.org> (accessed Jan 2018).

[44] M.J. Frisch, G.W. Trucks, H.B. Schlegel, G.E. Scuseria, M.A. Robb, J.R. Cheeseman, G. Scalmani, V. Barone, G.A. Petersson, H. Nakatsuji, X. Li, M. Caricato, A. Marenich, J. Bloino, B.G. Janesko, R. Gomperts, B. Mennucci, H.P. Hratchian, J.V. Ortiz, A.F. Izmaylov, J.L. Sonnenberg, D. Williams-Young, F. Ding, F. Lipparini, F. Egidi, J. Goings, B. Peng, A. Petrone, T. Henderson, D. Ranasinghe, V.G. Zakrzewski, J. Gao, N. Rega, G. Zheng, W. Liang, M. Hada, M. Ehara, K. Toyota, R. Fukuda, J. Hasegawa, M. Ishida, T. Nakajima, Y. Honda, O. Kitao, H. Nakai, T. Vreven, K. Throssell, J.A. Montgomery, Jr., J.E. Peralta, F. Ogliaro, M. Bearpark, J.J. Heyd, E. Brothers, K.N. Kudin, V.N. Staroverov, T. Keith, R. Kobayashi, J. Normand, K. Raghavachari, A. Rendell, J.C. Burant, S.S. Iyengar, J. Tomasi, M. Cossi, J.M. Millam, M. Klene, C. Adamo, R. Cammi, J.W. Ochterski, R.L. Martin, K. Morokuma, O. Farkas, J.B. Foresman and D.J. Fox, Gaussian 09 Revision E.01 2016, Gaussian Inc. Wallingford CT 2016.

[45] F. Zahariev, S.S. Leang and M.S. Gordon, J. Chem. Phys. **138** (24), 244108 (2013).

[46] T.H. Dunning Jr., J. Chem. Phys. **90** (2), 1007 (1989).

[47] R.A. Kendall, T.H. Dunning Jr. and R.J. Harrison, J. Chem. Phys. **96** (9), 6796 (1992).

[48] O. Christiansen, H. Koch and P. Jørgensen, J. Chem. Phys. **103** (17), 7429 (1995).

[49] H. Koch, O. Christiansen, P. Jørgensen, A.M. Sanchez de Meras and T. Helgaker, J. Chem. Phys. **106** (5), 1808 (1997).

[50] M. Schreiber, M.R. Silva-Junior, S.P.A. Sauer and W. Thiel, J. Chem. Phys. **128** (13), 134110 (2008).

[51] K. Andersson, P.Å. Malmqvist, B.O. Roos, A.J. Sadlej and K. Wolinski, J. Phys. Chem. **94** (14), 5483 (1990).

[52] K. Andersson, P.Å. Malmqvist and B.O. Roos, J. Chem. Phys. **96** (2), 1218 (1992).

[53] M.R. Silva-Junior, M. Schreiber, S.P.A. Sauer and W. Thiel, J. Chem. Phys. **129** (10), 104103 (2008).

[54] M.R. Silva-Junior, S.P.A. Sauer, M. Schreiber and W. Thiel, Mol. Phys. **108** (3), 453 (2010).

[55] M.R. Silva-Junior, M. Schreiber, S.P.A. Sauer and W. Thiel, J. Chem. Phys. **133** (17), 174318 (2010).

[56] M.J.G. Peach, P. Benfield, T. Helgaker and D.J. Tozer, J. Chem. Phys. **128** (4), 044118 (2008).

[57] T. Yanai, D.P. Tew and N.C. Handy, Chem. Phys. Lett. **393** (1-3), 51 (2004).

[58] H. Koch and P. Jørgensen, J. Chem. Phys. **93** (5), 3333 (1990).

[59] J.F. Stanton and R.J. Bartlett, J. Chem. Phys. **98** (9), 7029 (1993).

[60] M. Parac and S. Grimme, Chem. Phys. **292** (1), 11 (2003).

[61] S. Hirata, S. Ivanov, I. Grabowski and R.J. Bartlett, J. Chem. Phys. **116** (15), 6468 (2002).

[62] A. Dreuw, J.L. Weisman and M. Head-Gordon, J. Chem. Phys. **119** (6), 2943 (2003).

[63] D.J. Tozer, R.D. Amos, N.C. Handy, B.O. Roos and L. Serrano-Andrés, Mol. Phys. **97** (7), 859 (1999).

[64] M.E. Casida, C. Jamorski, K.C. Casida and D.R. Salahub, J. Chem. Phys. **108** (11), 4439 (1998).

[65] D.J. Tozer and N.C. Handy, J. Chem. Phys. **109** (23), 10180 (1998).

[66] C.A. Coulson and I. Fischer, Philos. Mag. **40** (303), 386 (1949).

Table 1: TDDFT (ω_{TDDFT}) and TDA (ω_{TDA}) excitation energies computed using the PBE, B3LYP, and SCAN exchange–correlation functionals, compared with reference values (taken from Refs. [22] and [55]). All values are in eV.

		PBE		B3LYP		SCAN		
	State	ω_{TDDFT}	ω_{TDA}	ω_{TDDFT}	ω_{TDA}	ω_{TDDFT}	ω_{TDA}	Ref
Local								
Acetamide	$^1\mathrm{A}''$	5.21	5.23	5.46	5.48	5.77	5.79	5.62
	$^1\mathrm{A}'$	6.59	6.68	7.04	7.13	7.27	7.36	7.14
	$^3\mathrm{A}''$	4.73	4.76	4.95	5.00	5.13	5.22	5.35
	$^3\mathrm{A}'$	5.21	5.29	5.24	5.42	5.28	5.52	5.71
Propanamide	$^1\mathrm{A}''$	5.23	5.25	5.49	5.51	5.79	5.81	5.65
	$^1\mathrm{A}'$	6.48	6.53	6.94	7.02	7.18	7.26	7.09
	$^3\mathrm{A}''$	4.76	4.79	4.98	5.03	5.16	5.24	5.38
	$^3\mathrm{A}'$	5.22	5.30	5.26	5.44	5.32	5.55	6.08
PAO-2	$^1\mathrm{B_u}$	5.51	5.92	5.63	6.00	5.67	6.09	6.18
	$^3\mathrm{B_u}$	3.04	3.25	2.89	3.25	—	2.54	3.38
PAO-3	$^1\mathrm{B_u}$	4.52	4.99	4.69	5.09	4.66	5.10	5.37
	$^3\mathrm{B_u}$	2.38	2.56	2.24	2.59	—	1.98	2.77
PAO-4	$^1\mathrm{B_u}$	3.86	4.32	4.06	4.44	3.99	4.41	4.81
	$^3\mathrm{B_u}$	1.99	2.14	1.85	2.20	—	1.65	2.41
PAO-5	$^1\mathrm{B_u}$	3.39	3.81	3.61	3.96	3.52	3.90	4.42
	$^3\mathrm{B_u}$	1.73	1.87	1.59	1.94	—	1.42	2.17
Naphthalene	$^1\mathrm{B_{3u}}$	4.24	4.25	4.44	4.46	4.42	4.45	4.38
	$^1\mathrm{B_{2u}}$	4.08	4.27	4.34	4.53	4.19	4.36	4.94
	$^3\mathrm{B_{3u}}$	3.83	3.87	3.95	4.00	*	3.77	4.18
	$^3\mathrm{B_{2u}}$	2.85	2.98	2.75	3.03	—	2.40	3.04
Charge–Transfer								
Model Dipeptide	$3^1\mathrm{A}'$	5.11	5.12	6.04	6.06	5.70	5.71	7.23
	$3^1\mathrm{A}''$	4.57	4.57	6.18	6.18	5.19	5.20	7.86
	$3^3\mathrm{A}'$	4.82	4.86	6.03	6.04	5.06	5.22	6.94
	$3^3\mathrm{A}''$	4.52	4.52	6.13	6.14	5.06	5.09	7.83
Rydberg								
CO	$1^1\Sigma^+$	9.09	9.11	9.80	9.82	9.92	9.92	10.73
	$2^1\Sigma^+$	9.40	9.40	10.13	10.14	10.12	10.12	11.34
	$2^1\Pi$	9.45	9.46	10.19	10.20	10.10	10.10	11.47
	$3^1\Sigma^+$	10.16	10.16	10.97	10.98	10.95	10.96	12.41
	$1^3\Sigma^+$	8.84	8.85	9.50	9.51	9.73	9.76	10.33
	$2^3\Sigma^+$	9.34	9.35	10.11	10.11	10.08	10.09	11.21
	$2^3\Pi$	9.39	9.39	10.16	10.16	10.07	10.07	11.37
	$3^3\Sigma^+$	10.13	10.13	11.01	11.01	10.75	10.78	12.34
N_2	$1^1\Sigma_g^+$	10.41	10.42	11.24	11.26	11.24	11.25	12.26
	$1^1\Pi_u$	10.76	10.76	11.65	11.65	11.46	11.46	12.88
	$1^1\Sigma_u^+$	10.66	10.66	11.62	11.62	11.30	11.30	12.93
	$2^1\Pi_u$	11.67	11.67	12.01	12.01	12.43	12.43	13.39
	$1^3\Sigma_g^+$	10.15	10.16	10.97	10.98	11.05	11.07	11.86
	$1^3\Pi_u$	10.74	10.74	11.66	11.66	11.46	11.46	12.83
	$1^3\Sigma_u^+$	10.63	10.63	11.60	11.60	11.28	11.29	12.83
	$2^3\Pi_u$	11.61	11.61	11.96	11.96	12.38	12.38	13.35

*Could not be calculated

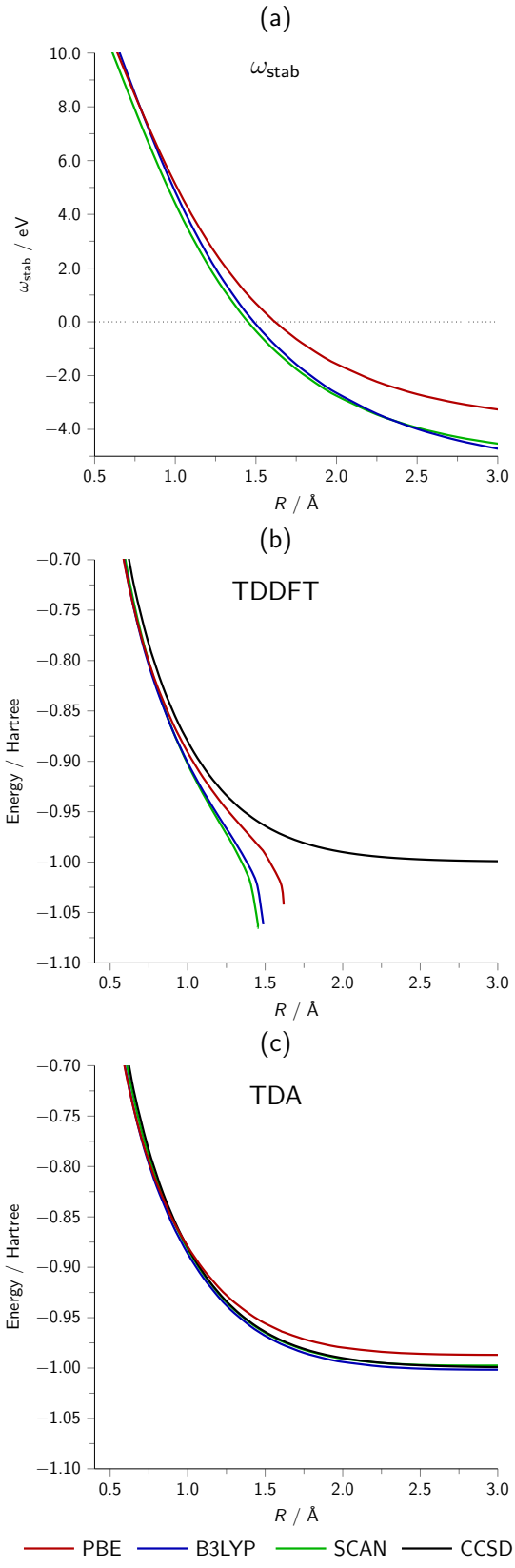

Figure 1: $^3\Sigma_u^+$ stabilities and potential energy curves in H_2.